ChemComm

View Online
Dynamic Article Links

Cite this: DOI: 10.1039/c1cc10389j

www.rsc.org/chemcomm

COMMUNICATION

Three-dimensional WO_3 nanostructures on carbon paper: photoelectrochemical property and visible light driven photocatalysis†

Xianghui Zhang,[a] Xihong Lu,[ab] Yongqi Shen,[a] Jingbin Han,[c] Longyan Yuan,[a] Li Gong,[d] Zhi Xu,[e] Xuedong Bai,[e] Min Wei,[c] Yexiang Tong,[b] Yihua Gao,[a] Jian Chen,[d] Jun Zhou*[a] and Zhong Lin Wang*[af]

Received 20th January 2011, Accepted 28th March 2011
DOI: 10.1039/c1cc10389j

Three-dimensional (3D) WO_3 nanostructures were grown on carbon paper by a catalyst-free high temperature reactive vapor deposition process, which exhibit a good photoelectrochemical property and visible light driven photocatalytic performance.

For the purpose of effectively utilizing the solar light or visible light, significant efforts have been focused on exploring new materials with band edge alignments suitable for driving the necessary photoelectrochemical and photocatalytic reactions.[1–4] It is now widely recognized that nanostructured semiconductors, in comparison to bulk materials, offer potential advantages in photoelectrochemical cells or photocatalytic applications due to their large surface area and size dependent properties, such as increased photon absorption, enhanced charge separation and migration, and surface reactions.[5,6] One-dimensional (1D) single crystalline structures are currently of great importance, as they can offer direct path for the photogenerated charges, with reduced grain boundaries, resulting in superior charge transport properties.[7–9]

Among transition metal oxides, tungsten trioxide (WO_3) has attracted considerable interests due to its promising physical and chemical properties.[10–12] WO_3 represents an important member of visible-light-driven photocatalysts, and has been demonstrated to exhibit high photocatalytic activity for the decomposition of organic compounds both in liquid and gas phase.[13–17] Moreover, WO_3 is recognized as one of the few *n*-type semiconductors resistant to photocorrosion in aqueous solutions, and has significant incident photo-to-current conversion efficiencies (IPCEs).[18] Recently, the study of visible-light-driven photoelectrochemical or photocatalytic properties of WO_3 nanostructures, including nanoparticles,[13] nanotubes[14] and nanorods[4] have attracted much attention due to their outstanding performances. In this work, we report the fabrication of three-dimensional (3D) WO_3 nanostructures on carbon paper *via* a high temperature reactive vapor deposition process. The photoelectrochemical measurement shows that the 3D WO_3 nanostructures have a strong photocurrent response under visible light illumination ($\lambda > 420$ nm). Moreover, they also exhibit a good visible light photocatalytic performance for the degradation of rhodamine B (RB).

The 3D WO_3 nanostructures were synthesized by a one-step, high temperature evaporation process by using tungsten powder as the source material in the presence of oxygen, which has been reported elsewhere (see the experimental section in ESI†).[19–22] After the evaporation deposition process, the color of the carbon paper substrate changed from dark grey to bright yellow. Fig. 1a and b show the scanning electron microscopy (SEM) images of carbon paper before and after the growth of WO_3 nanostructures, respectively. It can be seen that the carbon paper was woven by carbon fibers with the diameter of $\sim$10 μm. The carbon fibers were uniformly covered by the 3D WO_3 nanostructures after the growth process. The high yield of the product can be observed from the low magnification SEM image in Fig. 1c. The high-magnification SEM image in Fig. 1d clearly demonstrates the shape of the 3D nanostructure, which is constructed by intercrossed nanowires with the orientation of three perpendicular directions.

The crystal structure of the product was characterized by X-ray diffraction (XRD) measurement. According to Fig. 2a, all of the diffraction peaks, except two peaks of the carbon paper, can be indexed to monoclinic WO_3 (ICDD-PDF2-2004 cards: 01-072-0677). The dominant peak at 23.1°, 23.5° and 24.3° are corresponding to (002), (020) and (200) diffraction

[a] *Wuhan National Laboratory for Optoelectronics, and College of Optoelectronic Science and Engineering, Huazhong University of Science and Technology (HUST), Wuhan, 430074, China. E-mail: jun.zhou@mail.hust.edu.cn; Fax: +86-27-87792225; Tel: +86-27-87793105*
[b] *MOE of the Key Laboratory of Bioinorganic and Synthetic Chemistry, School of Chemistry and Chemical Engineering, Sun Yat-Sen University, Guangzhou, 510275, China*
[c] *State Key Laboratory of Chemical Resource Engineering, Beijing University of Chemical Technology, Beijing, 100029, P. R. China*
[d] *Instrumental Analysis & Research Center, Sun Yat-Sen University, Guangzhou, 510275, China*
[e] *Bejing National Laboratory for Condensed Matter Physics Institute of Physics, Chinese Academy of Sciences, Beijing, 100190, China*
[f] *School of Materials Science and Engineering, Georgia Institute of Technology, Atlanta, Georgia 30332-0245, USA. E-mail: zhong.wang@mse.gatech.edu; Fax: +1-404-894-8008; Tel: +1-404-894-9140*

† Electronic supplementary information (ESI) available: Experimental details, UV-vis absorption spectra of RB solution in the absence of the 3D WO_3 nanostructures, SEM images of the 3D WO_3 nanostructures after the dye degradation experiment. See DOI: 10.1039/c1cc10389j

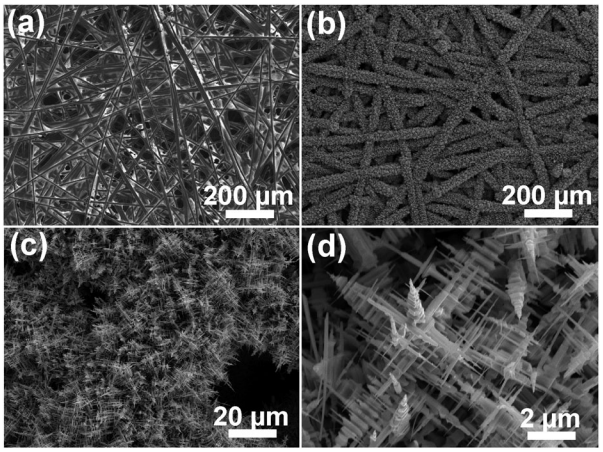

Fig. 1 (a) and (b) are SEM images of the carbon paper before and after the growth of 3D WO_3 nanostructures, respectively. (c) low-magnification and (d) high-magnification SEM image of the 3D WO_3 nanostructures, respectively.

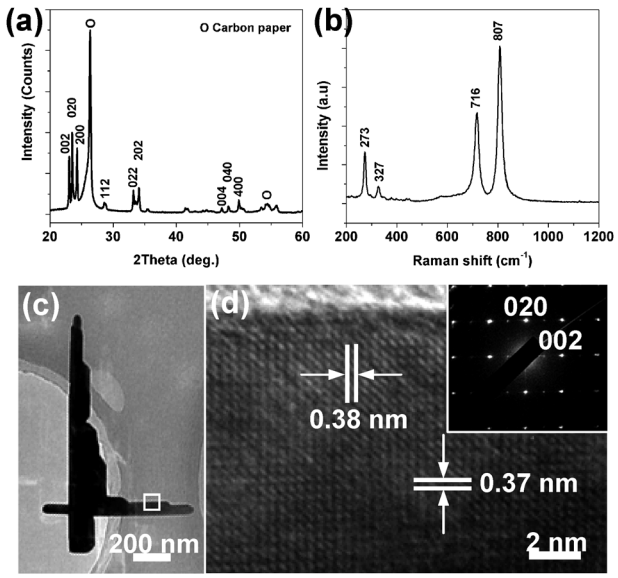

Fig. 2 (a) XRD pattern, (b) room temperature Raman spectrum, (c) low- magnification TEM image, and (d) HRTEM image of the 3D WO_3 nanostructures on carbon paper.

peak of WO_3, respectively. Fig. 2b displays a Raman spectrum of the 3D WO_3 nanostructures. The bands centered at 807 and 716 cm^{-1} arise from the W–O stretching, and the two bands located at 327 and 273 cm^{-1} belong to O–W–O bending modes.[23] The result indicates that the structure of the product is WO_3 monoclinic γ-phase.

Fig. 2c shows a low-magnification transmission electron microscopy (TEM) image of a broken 3D WO_3 nanostructures segment with a vertical cross junction. Corresponding selected area electron diffraction (SAED) pattern (inset in Fig. 2d) of the junction was recorded, proving the single crystalline nature of the whole junction. Fig. 2d displays a high-resolution transmission electron microscopy (HRTEM) image that was taken from the rectangle-closed area in Fig. 2c. Two sets of parallel fringes with the spacing of 0.37 nm and 0.38 nm were

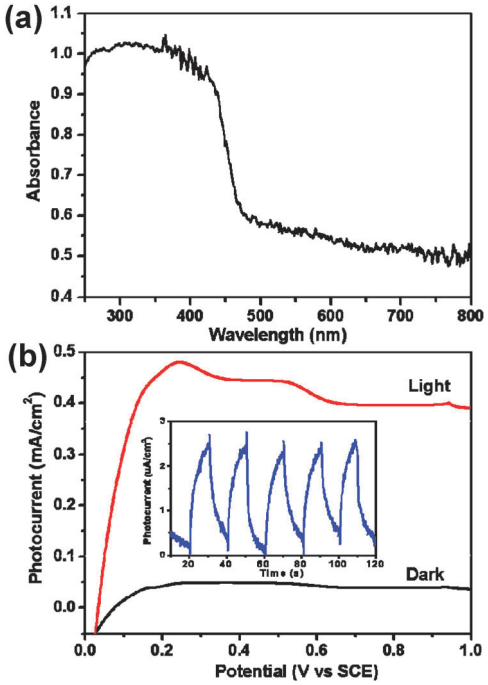

Fig. 3 (a) UV-vis absorption spectrum of 3D WO_3 nanostructures. (b) Current density *versus* potential (*J*–*V*) curve of 3D WO_3 nanostructures in the dark and under visible light irradiation (>420 nm). The inset shows the photocurrent response at zero bias.

obtained, correspond to the (020) and (002) planes of the monoclinic WO_3.

Fig. 3a shows the UV-visible absorption spectrum of the 3D WO_3 nanostructures. The optical band gap (E_g) of 3D WO_3 nanostructures can be calculated from the equation of $(\alpha h\nu)^2 = A(h\nu - E_g)$, where $h\nu$ is the photon energy, α is the absorption coefficient, and A is a material related constant.[24] The estimated E_g for the 3D WO_3 nanostructures is ~2.36 eV, indicating they are capable of capturing visible light. Hence, the photoelectrochemical cell (PEC) characterization of the 3D WO_3 nanostructures under visible light irradiation (>420 nm) was examined (see the experimental section in ESI†). Fig. 3b shows the photocurrent density *versus* potential (*J*–*V*) curve for the 3D WO_3 nanostructures in the electrolyte containing 0.1 M Na_2SO_4 both in the dark and under visible light irradiation. It can be clearly seen that the 3D WO_3 nanostructures exhibited a significant photocurrent density under visible light irradiation. The large photocurrent density of 0.45 mA cm^{-2} is observed with +0.25 V (*vs.* SCE). The inset in Fig. 3b is the photocurrent response to on-off cycling of the 3D WO_3 nanostructures recorded at zero bias. The steady and prompt photocurrent generation was observed during on and off cycles of illumination, demonstrating the good photocurrent stability under visible light irradiation.

In view of its visible photocurrent response, we further studied the visible photocatalytic activity of the 3D WO_3 nanostructures by photo-degradation of rhodamine B (RB) solution (see the experimental section in ESI†). To eliminate the self-degradation of RB and the substrate effect under irradiation, a carbon paper without WO_3 was also measured under the same conditions for comparison (the self-degradation

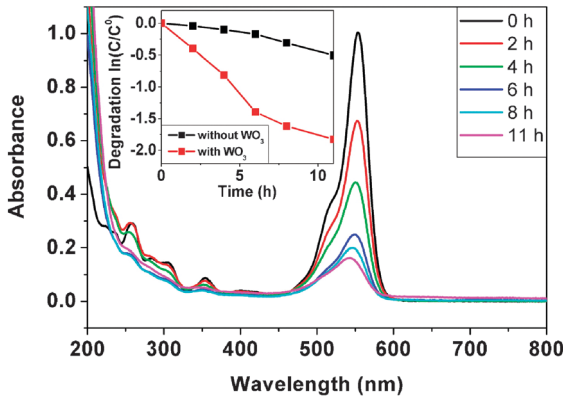

Fig. 4 UV-vis absorption spectra of RB solution as a function of irradiation time in the presence of 3D WO_3 nanostructures on carbon paper. Inset shows the plot of degradation $\ln(C_t/C_0)$ as a function of irradiation time.

of the RB solution with a slow rate is shown in Fig. S1 in ESI†). The decrease in the intensity of the absorbance band at ~560 nm is attributed to the decomposition of the RB solution. Fig. 4 shows the changes in the absorption spectra of RB solution after under visible light irradiation for 0 h, 2 h, 4 h, 6 h, 8 h and 11 h. It can be seen that 89% of the RB decomposed after 11 h visible light irradiation.

The inset of Fig. 4 is the plot of $\ln(C/C_0)$ *versus* irradiation time, where C and C_0 are the intensity of the absorbance peaks at 560 nm at the reaction time and the initial time, respectively. The initial solution concentration was purposely chosen to give an absorbance value of 1.0. The results reveal that the presence of the 3D WO_3 nanostructures catalyst increases the degradation process significantly. Moreover, it is worth noting that the 3D WO_3 nanostructures retained their original morphology and structure after the photodegradation reaction (See Fig. S2†), indicating the high stability of the 3D WO_3 nanostructures.

The enhanced photocatalytic ability and clear photocurrent response mentioned above can be attributed to its suitable band gap and the specific 3D structure. As indicated by the UV-visible absorption spectrum, 3D WO_3 nanostructures have a band gap of 2.36 eV that can absorb visible light. When 3D WO_3 nanostructures are irradiated by visible light, the photogenerated electrons and holes will be produced in the conduction band (CB) and valance band (VB) of WO_3, respectively. In our case, single crystalline 3D WO_3 nanorods can give an effective path for the electrons transport and thus suppress electron-hole recombination effectively. Furthermore, the 3D net structures grown directly on carbon paper not only can provide more active sites for the photoreaction, but also facilitate the species transport and electrons collection. Therefore, it is expected that the 3D WO_3 nanostructures in this work can be potentially used in the field of photoactive material.

In summary, 3D WO_3 nanostructures were synthesized on carbon paper by a catalyst-free high temperature reactive vapor deposition process. The visible-light-driven PEC and photocatalytic properties have been studied. The 3D WO_3 nanostructures exhibit a strong photocurrent response under visible light illumination ($\lambda > 420$ nm). In addition, a high visible light photocatalytic behavior for the decomposition of RB was also demonstrated. These results indicate that the 3D WO_3 nanostructures are promising candidate materials for PEC cell and photocatalysts for wastewater treatment.

ZXH and LXH contributed equally to this work. This work is supported by the National Natural Science Foundation of China (51002056, 51072236), the Program for New Century Excellent Talents in University (NCET-10-0397), a Foundation for the Author of National Excellent Doctoral Dissertation of PR China (201035). The authors thank the Analysis and Testing Center of Huazhong University of Science and Technology for support.

Notes and references

1 Y. H. Kim, H. Irie and K. Hashimoto, *Appl. Phys. Lett*., 2008, **92**, 182107.
2 M. G. Walter, E. L. Warren, J. R. McKone, S. W. Boettcher, Q. X. Mi, E. A. Santori and N. S. Lewis, *Chem. Rev*., 2010, **110**, 6446–6473.
3 Y. C. Nah, I. Paramasivam and P. Schmuki, *ChemPhysChem*, 2010, **11**, 2698–2713.
4 J. Z. Su, X. J. Feng, J. D. Sloppy, L. J. Guo and C. A. Grimes, *Nano Lett*., 2011, **11**, 203–208.
5 R. Van De Krol, Y. Liang and J. Schoonman, *J. Mater. Chem*., 2008, **18**, 2311–2320.
6 A. I. Hochbaum and P. D. Yang, *Chem. Rev*., 2010, **110**, 527–546.
7 M. Law, L. E. Greene, J. C. Johnson, R. Saykally and P. D. Yang, *Nat. Mater*., 2005, **4**, 455–459.
8 F. Qian, G. M. Wang and Y. Li, *Nano Lett*., 2010, **10**, 4686–4691.
9 G. M. Wang, X. Y. Yang, F. Qian, J. Z. Zhang and Y. Li, *Nano Lett*., 2010, **10**, 1088–1092.
10 I. Turyan, U. O. Krasovec, B. Orel, T. Saraidorov, R. Reifeld and D. Mandler, *Adv. Mater*., 2000, **12**, 330–333.
11 W. B. Cross and I. P. Parkin, *Chem. Commun*., 2003, 1696–1697.
12 M. Hepel, H. Redmond and I. Dela, *Electrochim. Acta*, 2007, **52**, 3541–3549.
13 Z. G. Zhao, Z. F. Liu and M. Miyauchi, *Chem. Commun*., 2010, **46**, 3321–3323.
14 Z. G. Zhao and M. Miyauchi, *Angew. Chem., Int. Ed*., 2008, **47**, 7051–7055.
15 M. Hepel and S. Hazelton, *Electrochim. Acta*, 2005, **50**, 5278–5291.
16 R. Abe, H. Takami, N. Murakami and B. Ohtani, *J. Am. Chem. Soc*., 2008, **130**, 7780.
17 C. Santato, M. Ulmann and J. Augustynski, *Adv. Mater*., 2001, **13**, 511–514.
18 C. Santato, M. Ulmann and J. Augustynski, *J. Phys. Chem. B*, 2001, **105**, 936–940.
19 J. Zhou, Y. Ding, S. Z. Deng, L. Gong, N. S. Xu and Z. L. Wang, *Adv. Mater*., 2005, **17**, 2107–2110.
20 X. Zhang, L. Gong, K. Liu, Y. Cao, X. Xiao, W. Sun, X. Hu, Y. Gao, J. Chen, J. Zhou and Z. L. Wang, *Adv. Mater*., 2010, **22**, 5292–5296.
21 J. Zhou, L. Gong, S. Z. Deng, J. Chen, J. C. She, N. S. Xu, R. S. Yang and Z. L. Wang, *Appl. Phys. Lett*., 2005, **87**, 223108.
22 Z. L. Li, F. Liu, N. S. Xu, J. Chen and S. Z. Deng, *J. Cryst. Growth*, 2010, **312**, 520–526.
23 D. Y. Lu, J. Chen, H. J. Chen, L. Gong, S. Z. Deng, N.S. Xu and Y. L. Liu, *Appl. Phys. Lett*., 2007, **90**, 041919.
24 X. Lu, D. Zheng, P. Zhang, C. Liang, P. Liu and Y. Tong, *Chem. Commun*., 2010, **46**, 7721–7723.